Quasi-diagonal reconstruction of Lyapunov spectra for spatio-temporal systems from multivariate time series

R. Carretero-González*, S. Ørstavik, and J. Stark
Centre for Nonlinear Dynamics and its Applications†,
University College London, London WC1E 6BT, U.K.
(PRELIMINARY VERSION, April 4, 2000, check http://www.math.sfu.ca/~rcarrete/abstracts.html for updates)

We use multivariate time-series generated by spatially extended systems to reconstruct their entire Lyapunov spectrum. Provided short range, or exponentially decaying, spatial interactions it is possible to approximately reconstruct the Jacobian by a banded matrix. Thus, by applying spatially localised reconstructions of the tangent space we estimate the whole Jacobian. This method circumvents the "curse of dimensionality" when trying to spatio-temporally embed the high-dimensional dynamics for extended dynamical systems. The technique is illustrated using coupled map lattices as prototype models for spatio-temporal chaos.

PACS numbers: 05.45.Ra, 05.45.Jn, 05.45.Tp

Contents

I. INTRODUCTION

One of the most important tools for investigating chaotic dynamical systems are the Lyapunov exponents. The Lyapunov exponents typically measure the average exponential divergence of two infinitely close orbits. In this manuscript we are interested in extracting *all* the Lyapunov exponents of spatio-temporal systems without prior knowledge of the dynamical equations and where solely a multivariate time-series from the system can be measured. The negative (or at least some of the first negative) Lyapunov exponents are extremely useful since they are needed for estimating the dimension of the attractor through the Kaplan-Yorke conjecture.

The extraction of all the Lyapunov exponents from time series for extended dynamical systems is a daunting task. The problem resides in the high dimensionality of the system where any attempt to embed the high-dimensional attractor fails due to the well-known "curse of dimensionality". In this manuscript we present a method for extracting Lyapunov exponents for spatio-temporal systems. The method is based on only reconstructing the non-zero entries of the Jacobian in a row-by-row fashion. For extended dynamical systems, coupled by local interactions, each row of the Jacobian only possesses a few non-zero elements near the diagonal. Thus our implementation relies on a row-by-row low-dimensional reconstruction and hence avoids the "curse of dimensionality". It is worth commenting that in some cases it is possible to give a reasonable reconstruction, in terms of prediction error, using a quite low dimensional spatio-temporal embedding dimension [1]. This apparent counter intuitive result may be explained by the rapid decay on the dependence of neighbouring dynamics [2].

During the preparation of this manuscript we became aware of the work by Bünner and Hegger [3] were they carry out a similar treatment as the one presented here. Their focus is rather different in that they use an approach based on Lyapunov exponents for non-autonomous systems. They only present results for a coupled logistic lattice using a linear fitting basis. Our analysis is more complete in that we consider more general local maps (skewed logistic map) with a more flexible, quadratic, fitting basis. More importantly, we also provide the methodology to apply our approach to more general coupling schemes (*i.e.* with larger range of interaction) and we give numerical results to exemplify our findings. This development allows for a straightforward extension of the quasi-diagonal reconstruction for continuous space-time extended dynamical systems (cf. PDEs). Another point that we further address is the importance of truncating the outer layer(s) of the Jacobian to avoid boundary effects. We have already raised this point in a previous paper [4]. The present work combines the best features introduced in references [3] and [4] with additional generalisations and extensive supporting numerical evidence. Nonetheless, the present manuscript is presented in a self contained manner. The sectioning presented here provides the different steps in a natural progression towards the reconstruction of the dynamics for spatially extended systems. We begin with univariate analysis and end with a successful quasi-diagonal reconstruction of the Jacobian from multivariate time series. In the process we highlight the interrelation between the 'globality' of our fitting basis and the "curse of dimensionality". We also pinpoint the importance of properly addressing the effects on the boundaries of the subsystem (spatial window where we collect the multivariate time series) under consideration.

This manuscript is organised as follows. Next section is devoted to give a general introduction on spatio-temporal systems and to introduce the prototype model (coupled map lattice) that we are going to investigate. In section III we give quick overview on Lyapunov spectra for extended dynamical systems and their relevance. We give some examples and explain how to estimate the Lyapunov spectra using subsystem information through a suitable rescaling. In section IV we attempt to reconstruct the dynamics using univariate time series. The lack of sufficient spatial information hinders any attempt of performing a decent reconstruction when using standard univariate (temporal) delay embeddings for spatio-temporal systems. In section V we give a systematic study of attempting to reconstruct Lyapunov spectra using different spatio-temporal embeddings. We stress the importance of including spatial information in order to obtain sensible reconstructions. We also point out that the boundary effects on the the measured subsystem have to be properly addressed by a truncation of the outer layer(s) of the reconstructed Jacobian. In section VI we turn our attention to the effect of going from a local fit to a global fit when increasing the dimension of the spatio-temporal embedding. We conclude that the "curse of dimensionality" suppresses any hope of a decent reconstruction when our fitting basis does not give a good global approximation to the dynamics. In section VII we exploit the spatial homogeneity and the finite coupling interaction range of the coupled map lattice to develop a novel technique to reconstruct Lyapunov spectra for spatio-temporal systems. This method circumvents both: the problem of the "curse of dimensionality" and the error induced by not having an appropriate global basis. Section VIII is devoted to the generalisation of the technique for systems with spread, though exponentially localised, coupling interactions. Finally, in the last section, we provide a natural extension of our method for its application in PDEs.

II. SPATIALLY EXTENDED SYSTEMS

The occurrence of chaos in spatio-temporal systems has recently attracted the attention of a large part of the dynamical systems community. There exists nowadays a very broad understanding of low-dimensional chaotic systems. However, the same cannot be said of high-dimensional systems and in particular for spatially extended dynamical systems. The addition of an spatial extent to the dynamics produces a complex interplay between the local dynamics (original dynamics before including spatial interactions) and the spatial interactions. Sometimes, this interplay triggers the so called spatio-temporal chaos. In a spatio-temporal chaotic regime both space a time evolutions suffer from instabilities and it is even possible to quantify spatial and temporal Lyapunov exponents [5]. Loosely speaking, spatio-temporal chaos refers to the usual temporal chaotic evolution with an extra decay on spatial correlations. A possible simple mechanism to achieve spatio-temporal chaotic motion is to spatially couple low-dimensional chaotic units — although one has to be careful because the coupling sometimes tends to reduce the spatio-temporal instabilities [6]. However, it is possible to produce spatio-temporal evolution through the spatial interaction of well-behaved (non-chaotic) units —this is the case for some metapopulation dynamics models [7].

In contrast with non-spatially distributed systems, spatio-temporal systems posses a spatial support. This support may be given in terms of a spatial pinning of dynamical units in a discrete lattice or by means of a dependence on continuous spatial variables. The typical model for continuous space and time spatio-temporal systems consists of partial differential equations (PDE). By discretising space the system reduces to a lattice of ordinary differential equations commonly referred as lattice differential equations (LDE). In the discrete space case, the system can be viewed as a collection of low dimensional dynamical systems coupled together via some spatial rule (for a review on current research please see [8]). Examples for this kind of models are abundant in the literature, particularly in the field of solid state physics where they are *ad hoc* for the study of interacting atoms arranged in some lattice configuration, see Ref. [9] and references therein.

In this paper we focus our attention on a third category of extended dynamical systems where not only space is discrete but time is taken to be discrete as well. In such a case the model consists of low-dimensional dynamical units with discrete time (*i.e.* maps) arranged in some discrete lattice configuration in one or more dimensions. These models are the so-called coupled map lattices (CML). Coupled map lattices where first introduced in 1984 as simple models for spatio-temporal complexity [10–12]. Despite their computational simplicity, CML are able to reproduce a wide range of spatio-temporal behaviour such as intermittency [13], turbulence [14,15] and pattern formation [16], to name just a few.

Formally, for the one-dimensional case, let us consider a one-dimensional array of sites. The length of the array could be infinite but for the purpose of the present study we consider an array of length N with periodic boundary conditions. At the i-th site we introduce a real dynamical variable x_i and a time-discrete local dynamical system —the *local map* f. For the simplest case, the local variable x_i and the local map f are taken to be one-dimensional. We suppose that the same local map f acts at every spatial location (homogeneous local dynamics). The dynamics of the CML is then a combination of local dynamics and coupling, which consists of a weighted sum over some neighbourhood. The time-evolution of the i-th variable is given by

$$x_i^{n+1} = \sum_k \varepsilon_k f(x_{i+k}^n), \tag{1}$$

where the range of summation defines the neighbourhood. The coupling parameters ε_k are site-independent, and they satisfy the conservation law $\sum \varepsilon_k = 1$, to prevent unboundedness as time increases to infinity. The most common choice for the coupling scheme is

$$x_i^{n+1} = (1-\varepsilon) f(x_i^n) + \frac{\varepsilon}{2}\left(f(x_{i-1}^n) + f(x_{i+1}^n)\right), \tag{2}$$

which is called *diffusive* CML. The diffusive CML corresponds to the discrete analogue of the reaction-diffusion equation. There is now a single coupling parameter ε which is constrained by the inequality $0 \le \varepsilon \le 1$, to ensure that the sign of the coupling coefficients in (2) (*i.e.* $\varepsilon/2$ and $1-\varepsilon$) remain positive.

III. LS FOR EXTENDED DYNAMICAL SYSTEMS

Let us now give an overview on the extraction and application of Lyapunov spectra for spatio-temporal systems. For a N-dimensional dynamical system there exist N Lyapunov exponents which in principle can be obtained from the eigenvalues of the matrix

$$\Gamma = \lim_{n\to\infty} \left[P(n)^{\mathrm{tr}} \cdot P(n)\right]^{1/2n}, \tag{3}$$

where $P(n)$ corresponds to the product of the first n Jacobians along the orbit and we use $(\,\cdot\,)^{\mathrm{tr}}$ to denote matrix transpose. The Lyapunov exponents are then defined as the logarithms of the eigenvalues of Γ. The procedure defined by equation (3) seems straightforward enough to be applied in practice provided the limit converges fast enough. However, multiplying the Jacobians produces an ill-conditioned problem since the most expanding direction swamps all the other expansion/contraction rates. Therefore one has to recur to algorithms that reorthogonalise the matrix product of the Jacobians. Such algorithms are based upon Graham-Schmidt (GS) orthogonalisation [17]. An alternative method to compute the eigenvalues of Γ is to use the so-called HQR decomposition that uses Householder transformations to split matrices onto the product QR, where R is an upper triangular matrix and Q is an orthonormal matrix (all rows/columns are orthonormal to each other). We in fact use an efficient HQR method to compute Lyapunov exponents described in Ref. [18] where only the relevant operations for the computation of the Lyapunov exponents are carried out.

We finally define the Lyapunov spectrum (LS) as the set of Lyapunov exponents $\{\lambda_i\}_{i=1}^N$ arranged in decreasing order. The LS is a very useful characterisation not only because it gives the expansion/contraction rates of infinitesimal changes, but also because estimates of dimension and entropies of the system can be inferred from it. An estimation of the dimension of the chaotic attractor, equivalent to the effective number of degrees of freedom, is given by the Kaplan-Yorke conjecture [19] through the *Lyapunov dimension* D_L defined as

$$D_L = j + \frac{1}{|\lambda_{j+1}|}\sum_{i=1}^{j} \lambda_i, \tag{4}$$

where j is the largest integer for which $\sum_{i=1}^j \lambda_i > 0$. It is also possible to extract from the LS an upper bound for the so-called *Kolmogorov-Sinai* (KS) *entropy* h by the following approximation [20]

$$h = \sum \lambda_i^+, \tag{5}$$

where the summation is over the positive Lyapunov exponents λ_i^+. The KS entropy is a useful concept in that it quantifies the mean rate of information production in a system, or alternatively the mean rate of growth of uncertainty due to infinitesimal perturbations.

As an example we depict in figure 1.a the LS for a coupled logistic lattice of size $N = 20$ with periodic boundary conditions obtained using the known dynamics (2). In figure 1.b we plot the sum of the Lyapunov exponents $\sum_{k=1}^i \lambda_k$ from where the KS entropy can be estimated (maximum of the curve) and the Lyapunov dimension can be extracted (intersection with the horizontal axis). It is interesting to notice that the Lyapunov dimension $D_L \simeq 15.4$ is comparable to the total size of the lattice $N = 20$. Also notice that $D_L \simeq 15.4$ implies the presence of a high dimensional attractor. This point will be addressed in more detail in the following sections.

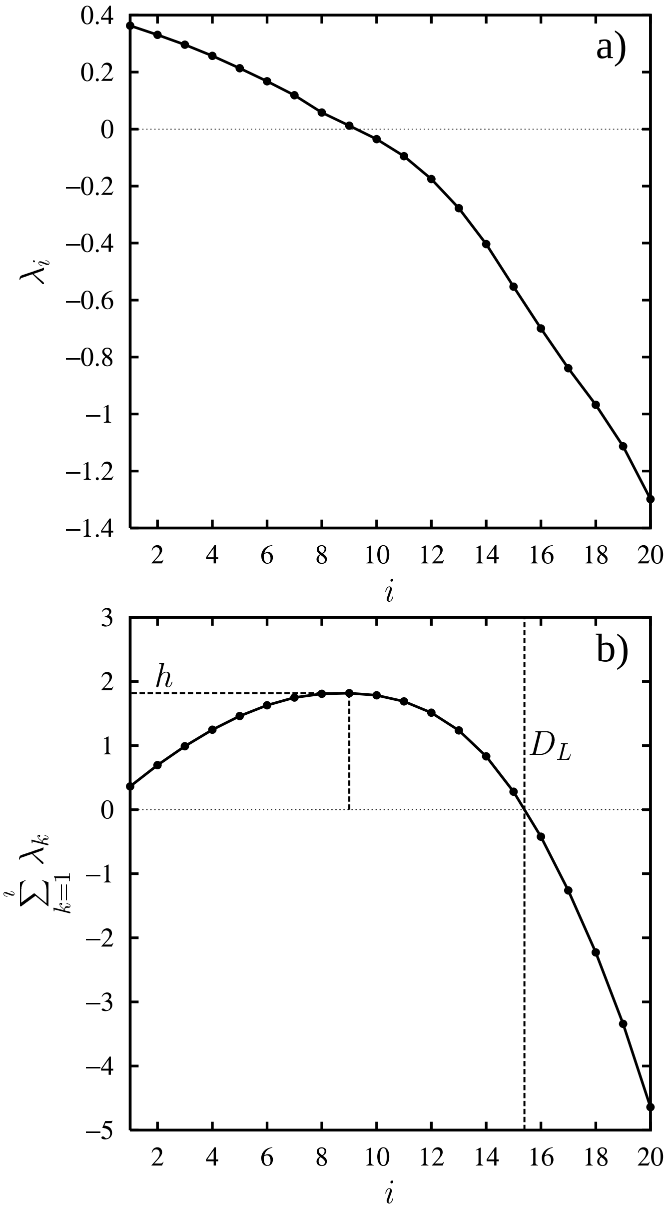

FIG. 1. a) Lyapunov spectra for a CML of $N = 20$ fully chaotic logistic maps $f(x) = 4x(1-x)$ with coupling strength $\varepsilon = 0.4$. b) The Lyapunov dimension D_L and the KS entropy h may be estimated from the sum of the Lyapunov exponents. In this case the largest Lyapunov exponents is $\lambda_1 \simeq 0.36$, $D_L \simeq 15.4$ and $h \simeq 1.8$.

It is important to mention that the computation of the whole LS for spatio-temporal systems is a cumbersome task as the system size gets larger. As described above, in order to obtain the whole LS one has to employ numerical methods involving some matrix manipulations of the Jacobians. These methods, even the most efficient ones, typically involve, for a system of size N, a number of step proportional to N^3 [17]. For medium lattice sizes ($N < 50$) the number of operations, per time step, involved is already considerable. Moreover, taking into account that sometimes the (time) convergence of the Lyapunov exponents is extremely slow, the time necessary to compute the whole LS for spatio-temporal systems quickly becomes prohibitive. Furthermore, it is often desirable to think about the thermodynamic limit of the system, namely when the limit of infinite lattice size in assumed. For such a case —infinite number of Lyapunov exponents— it is impossible to compute the whole LS and one has to resort to subsystem LS rescaling techniques that we now briefly describe.

In order to describe the rescaling of subsystem LS let us consider a one-dimensional lattice of coupled one-dimensional dynamical units. High dimensional cases may be treated in a similar way. Consider the array to be large in size ($N \gg 1$) and suppose for the time being that it is constituted by smaller *independent* subsystems of size N_s —for simplicity suppose that N is a multiple of N_s. The LS of the whole lattice, in the case of uncoupled subsystems, corresponds to N/N_s exact copies (if we assume spatial homogeneity) of the same LS containing N_s Lyapunov exponents. Thus, the LS for this whole lattice consists of N_s Lyapunov exponents with multiplicity N/N_s. When these subsystems are uncoupled, provided that they are large enough, they will reflect approximatively the dynamics of a large, fully coupled, lattice. As we relax the assumption of independent subsystems and consider the original lattice, we hope that the LS is not significantly modified [21,22]. If this is true, the whole LS of the original lattice may be approximated by a rescaled version of its subsystem LS. An obvious choice for the rescaling would be to multiply the index i of the N_s-subsystem Lyapunov exponents $\lambda_i(N_s)$ by $r' = N/N_s$. However, careful analysis of the LS of homogeneous evolution suggests that a better rescaling is achieved by using the rescaling

$$r = \frac{N+1}{N_s+1}. \tag{6}$$

In fact this new rescaling factor improves considerably the rescaling method. For a detailed analysis on this new rescaling method please see Ref. [23].

The rescaling of the whole LS from subsystem information leads us naturally to define intensive quantities from extensive quantities. As a direct consequence of this rescaling —using the same argument as in the previous paragraph— it is straightforward to see that the Lyapunov dimension and the KS entropy are extensive quantities (D_L and h increase linearly with N). Moreover, it is useful to introduce their respective densities by simply dividing them by the system volume (lattice size) [24]. By doing so, the LS, Lyapunov dimension and KS entropy could be defined through densities and no restriction on the original size of the system is necessary. Thus, the densities could even be defined for the thermodynamic limit —however it is a delicate matter for infinite dimensional systems such as in PDEs [25]. Therefore, by using the rescaling of subsystem LS, one can considerably reduce the computing resources (running time and memory allocation) needed to estimate the whole LS of a large spatio-temporal system. Furthermore, by restricting ourselves to information in a subsystem one reduces the dimensionality of the observed data and thus it is possible to apply embedding reconstruction ideas more naturally.

IV. LS FROM UNIVARIATE TIME SERIES

In the previous section we focused on the extraction of the whole LS of an extended dynamical system from which the dynamics is known. From now on, we would like to perform this task when the only information accessible about the system is through its time series. Let us start by applying the standard delay embedding technique from a single observable time-series.

Takens embedding theorem [26] provides the formal justification that a *univariate* (one-dimensional) time series generically contains all the coordinate-free properties of a dynamical system. This time series need not to be the time history of one of its dynamical variables but it can be a generic observable function non-trivially dependent on all/some of the variables of the system. In particular, it is possible to reconstruct, in principle, all the Lyapunov exponents of a given orbit from a univariate time series. Positive Lyapunov exponents are, typically, relatively easy to reconstruct from the time series. By relatively easy we mean that the typical amount of data required is quite manageable. However, negative Lyapunov exponents are, most of the time, very difficult to approximate even for low-dimensional systems. The problem resides in the fact that the attractor becomes very 'thin' along the contracting directions and thus a lack of available data arises.

It is important to clarify that Takens embedding theorem does not strictly apply to the choice of models and observations used throughout this manuscript. Takens embedding theorem fails for CMLs for a number of reasons, in particular any observation function (univariate or multivariate) is far from being generic unless we measure *all* the system's variables [1]. However, it has been shown that using spatio-temporal delay embeddings in dimensions as low as $d = 4$ give considerably low prediction errors [1]. Therefore, even that the strict requirements of Takens embedding theorem are not satisfied here, we will continue to use spatio-temporal delays to obtain the reconstructed LS.

The reconstruction of the dynamics from time series is based upon time delay reconstruction. Suppose that the univariate time series $\{\varphi_n\}$ has been measured from a N dimensional system and construct from it the series of delay vectors defined by

$$y_n = (\varphi_n, \varphi_{n-1}, \ldots, \varphi_{n-(d-1)}), \tag{7}$$

where d is the so-called *embedding dimension*. Takens [26] showed that, for large enough d, the dynamics induced on the delay vectors is generically a smooth conjugacy of the original dynamics. However, Takens embedding theorem does not give the means to characterise this smooth coordinate change and thus it is impossible to exactly reconstruct the original dynamics (in its original coordinate system). That is the reason why only coordinate-free properties can be reconstructed from time series. In particular it is worth recalling that the Lyapunov exponents are invariant under smooth coordinate changes and thus it is possible to apply delay embedding reconstruction to recover the LS from time series.

A crutial point when applying delay embedding is the choice of embedding dimension d. Takens showed that is suffices that

$$d \geq 2k + 1, \tag{8}$$

where k is the dimension of the k-dimensional manifold where our system is embedded. This apparently arbitrary condition is a simple geometrical disentangling in order to avoid self intersections on the reconstructed manifold [27]. For the extended dynamical systems we are considering, k would be the actual number of dynamical units in the lattice times the dimension of the local dynamics. For the case we are interested one, *i.e.* a one-dimensional array of N sites with a one-dimensional local map at every node, we get $k = N$. Thus for large N an embedding dimension of $2N+1$ is clearly unpractical. Currently, Sauer and Yorke are working on a similar bound as in (8) where the new (more relaxed) estimate for the embedding dimension, in order to preserve box-counting dimension and Lyapunov exponents, is given by

$$d > D_B + D_T, \tag{9}$$

where D_B is the box-counting dimension of the attractor and D_T is the "tangent dimension". The tangent dimension is, essentially, the maximum (over all points) dimension of the tangent space of the underlying dynamics [28]. Nevertheless, even using the new estimate (9) for d, the dimensions involved when reconstructing spatio-temporal dynamics are still prohibitive. For example, from the results presented in the previous section (cf. figure 1), the Lyapunov dimension for a quite small lattice of $N = 20$ coupled logistic maps is approximately $D_L = 15.4$. Then, by using the Kaplan-Yorke conjecture, the estimate (9) would read $d > 15.4 + D_T$. Therefore, no matter how small D_T turns out to be, the embedding dimension for this small lattice would have to be larger than $D_L = 15.4$.

Let us now discuss briefly the immediate and unavoidable problem when dealing with large embedding dimensions, *i.e.* the so-called "curse of dimensionality". Provided a right choice of embedding dimension, the delay vectors in equation (7) reconstruct, up to a smooth coordinate change, the dynamics of the original system. In order to estimate the LS from the time series we need to approximate the map that governs the dynamics of the delay vectors —that is the map F such that $F(y_n) = y_{n+1}$. This map F is a smooth conjugate of the original dynamics and thus preserves the Lyapunov exponents of the latter. There exist several methods to approximate this map based on local approximations. This techniques rely on scanning the time series to find a set of past close encounters (neighbours) of the current reconstructed state. Once these neighbours have been found, an approximation $\hat{F}$ for the map F at the chosen point can be computed using, for example, least squares. For a comprehensive review on delay embedding reconstruction methodology with practical applications and explicit algorithms we recommend the recent book by Kantz and Schreiber [29]. For large embedding dimensions ($d \sim 6$) it becomes extremely difficult to find close neighbours and hence, due to data limitations, the approximation of F is not longer local. Therefore the errors in determining $\hat{F}$ induce large inaccuracies in the determination of the Lyapunov exponents for large embedding dimensions.

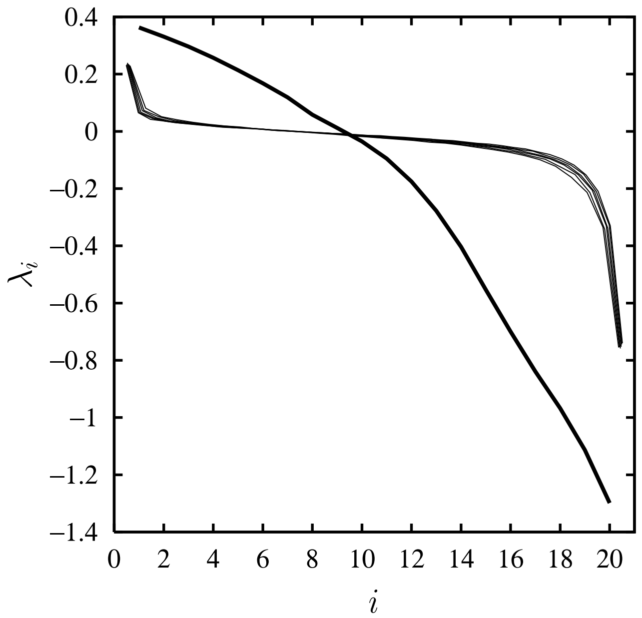

FIG. 2. Time delay embedding reconstructions of the LS for a logistic coupled map lattice of size $N = 20$ and coupling $\varepsilon = 0.4$ using univariate time series. The LS computed from the original dynamics is depicted with a thick line. The time delay reconstruction of the LS from a single univariate time series is shown with the thin lines for even delay embedding dimensions $d \in [32, 42]$. We used a second order fitting from a sample of 10^4 points and we set the number of neighbours to be the number of parameters in the fitting process fit plus 20. The LS was reconstructed from estimating the Jacobians over 10^4 iterations. We also used the rescaling (6) introduced in Ref. [23] to rescale the reconstructed LS.

It is clear then that delay embedding techniques are bound to fail when reconstructing spatio-temporal systems where the dynamics is typically high dimensional. As an example we depict in figure 2 an attempt to estimate the whole LS from a univariate time series obtained from a single site of a couple logistic lattice. The measurement function in this case is the projection onto a single site. Namely, the entries of the delay vectors (7) are chosen to be $\varphi_n = x_j^n$ for a fixed j. We used temporal delays d in the range $32 \leq d \leq 42$. It is obvious from the figure that this temporal delay reconstruction of the LS (overlapping thin lines) completely fails to reproduce the LS of the original system (thick line) —note that even the trend of the curve is not similar. Other variants of the reconstruction parameters briefly mentioned in the figure caption where also tried yielding to the same qualitative results. We even tried embedding dimensions satisfying the condition (8) without obtaining any improvement in the LS reconstruction.

V. LS FROM SPATIO-TEMPORAL DATA

Since the direct application of univariate (temporal) delay embeddings reconstructions clearly fails for spatio-temporal systems, let us now try to exploit the spatial extent of the dynamics and use spatio-temporal delay embeddings. The framework for spatio-temporal delay embeddings is presented in Ref. [1]. In this section we show the relevance of including the spatial information in the measured time series and stress the importance of truncating the outer layer of the reconstructed Jacobians in order to avoid boundary effects. We have already addressed these issues in a previous paper [4], however we include here some of the analysis for completeness.

Consider now, instead of the delay vectors (7) of the previous section with $\varphi_n = x_j^n$, the following *spatio-temporal* delay vectors

$$y_i^n = (\phi_i^n, \phi_{i-1}^n, \ldots, \phi_{i-(d_s-1)}^n), \tag{10}$$

whose entries $\phi_i^n = (x_i^n, x_i^{n-1}, \ldots, x_i^{n-(d_t-1)})$ are time-delay vectors and the index i is fixed. The overall embedding dimension for this spatio-temporal embedding is $d = d_s d_t$, where d_s and d_t denote, respectively, the spatial and temporal embedding dimensions. The usual temporal delay embedding is recovered by setting $d_s = 1$. Spatio-temporal embedding techniques have proved useful in various cases [30–32]. When adding the extra spatial delay in the time series one is including important information that is otherwise very difficult to obtain. In fact, it is extremely difficult to extract information of neighbouring dynamics by just doing spatially localised measurements. This is because the rapid decay of spatial correlations in locally coupled extended dynamical systems (cf. diffusive CML). In a previous paper [2] we showed how this extremely rapid decay in correlations allows a quite small truncated lattice with random input at the boundaries to reproduce the local dynamics (equivalent to a univariate time series using pure temporal embeddings) of a large, potentially infinite, lattice. This would tend to suggest that univariate time series cannot typically reconstruct in practice the dynamics of a whole spatio-temporal system.

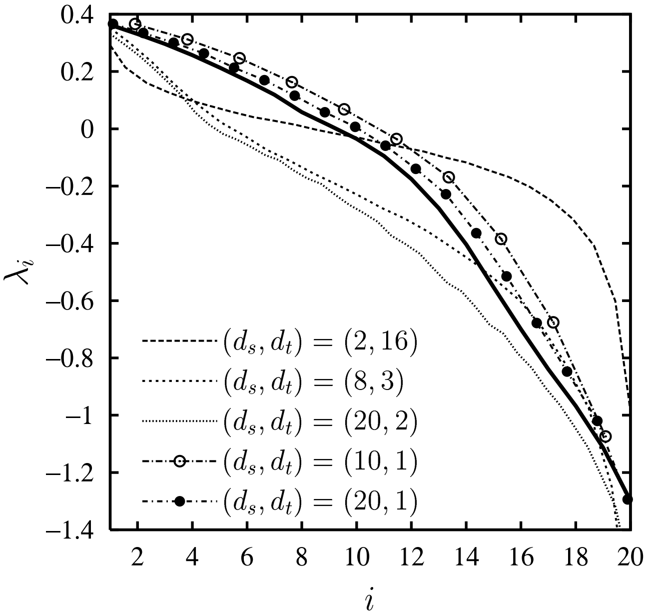

FIG. 3. Spatio-temporal delay embedding reconstructions of the LS for a logistic coupled map lattice. The LS computed from the original dynamics is depicted with a thick line while the different spatio-temporal delay reconstructions are depicted with the dashed lines. All the fitting parameters are the same as in figure 2 (second order fitting, 10^4 points).

In figure 3 we depict several attempts to reconstruct the LS of the coupled logistic lattice (as in figure 2) for different spatio-temporal embedding dimensions. The different reconstructions correspond to a broad sample of choices of d_s and d_t. It is crutial to note that the sole fact of increasing $d = d_s d_t$ does not improve the estimates of the LS. In fact, in order to get a good estimate of the LS, it seems more important to take $d_t = 1$ and d_s as large as possible. This is depicted by the empty and filled circles corresponding to $d_t = 1$ and $d_s = 10$ and $d_s = 20$ respectively. In the figure we show a few combinations for (d_s, d_t), however we originally considered a much broader choice without any qualitative difference. Therefore, a spatio-temporal reconstruction with $d_t = 1$ —corresponding to a pure *spatial* delay embedding— seems to give the best results. This result is easy to explain since we are using the actual dynamical variables of the system ($\varphi_i^n = x_i^n$) as observables and we are measuring them in a complete window. Thus, we do not need to increase the embedding dimension to avoid self intersection in the reconstructed space since we are already in the natural space for the system.

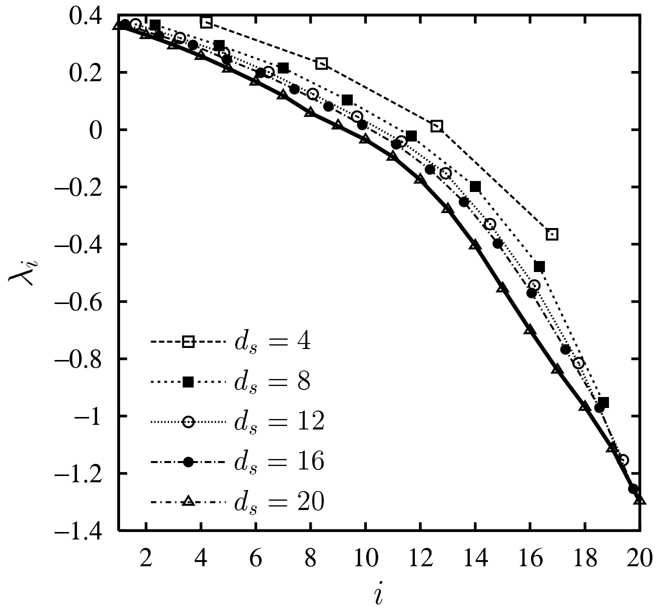

FIG. 4. Pure spatial delay embedding reconstructions of the LS for a logistic coupled map lattice. All the fitting parameters are the same as in figure 2 (second order fitting, 10^4 points).

In figure 4 we depict the reconstruction of the LS using pure spatial embedding for increasing d_s in order to get better estimates as suggested by figure 3. For the pure spatial embedding ($d_t = 1$) the reconstructions for the LS are much more promising than before. It is interesting to mention that since our original system is of size $N = 20$ it is not possible to choose $d_s > 20$ for any d_t. Indeed, we have to be careful since taking $d_t = 1$ and $d_s = N = 20$ corresponds to measuring the *whole* state space and not to an embedding reconstruction. This explains why the reconstructed LS for $d_t = 1$ and $d_s = N = 20$ perfectly agrees with the direct computations (see triangles in figure 4).

From figure 4 we can observe that as d_s is increased a better approximation for the LS is achieved. One may think that this is simply the effect of getting a higher embedding dimension. However, the reason for the apparent convergence of the reconstructed LS towards the exact LS as $d_s \to N$ is simply due to a reduction of the noise from boundary effects. Consider the sites at the boundary of our spatial window where we extracted the multivariate time series. The dynamics of these sites depends on sites whose evolution is *not* explicitly contained in the measuring window. As a consequence, the estimation of the Jacobian for these sites contains spurious information and is plagued with errors. For the $(d_s, d_t) = (20, 1) = (N, 1)$ case (triangles in figure 4), since we have *all* the variables of the system there are no such errors and the estimation of the LS is perfect.

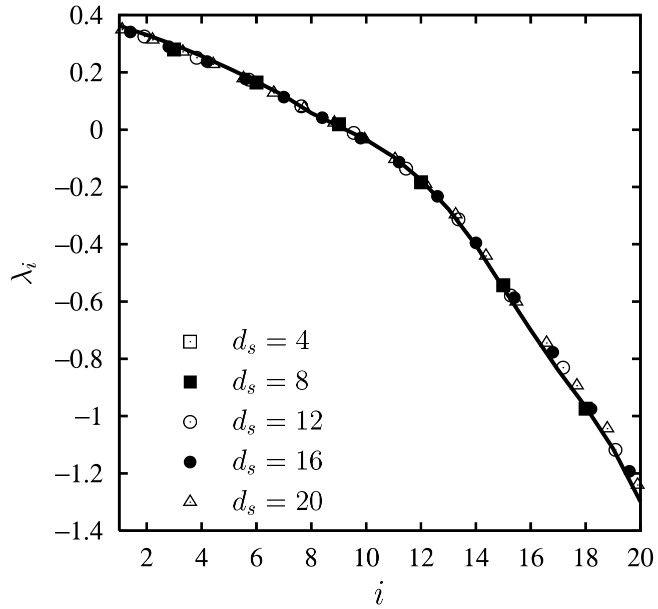

FIG. 5. Pure spatial delay embedding reconstructions of the LS for a logistic coupled map lattice. In contrast with figure 4, here we truncate the outer layer of the reconstructed Jacobian. All the fitting parameters are the same as in figure 2 (second order fitting, 10^4 points).

In order to avoid the boundary effects when the measuring window does not cover all the variables of the system we need to notice that the boundary sites contribute towards the Jacobian at its outer rows and columns. In order to get rid of the boundary effects we simply truncate the outer rows and columns of the reconstructed Jacobian. The resulting truncated Jacobian is a $(d_s - 2) \times (d_s - 2)$ matrix. It is important to notice that one must first fit the $d_s \times d_s$ Jacobian and only then truncate its outer rows and columns. For instance, if one does not remove the outer layer of the Jacobian, the fitting procedure of the first raw will include unwanted non-zero terms off the tri-diagonal. This non-zero elements arise from the lack of information from the left neighbouring site that is outside of our measuring window and thus the fitting algorithm tries to compensate by including an artificial dependence on *all* sites inside the window.

Therefore, for a spatial delay embedding dimension d_s we obtain a $(d_s-2)\times(d_s-2)$ reconstructed Jacobian and thus $d_s - 2$ Lyapunov exponents. The results of applying this technique are depicted in figure 5. This figure must be compared to 4 where the outer layer of the Jacobian was not truncated. The estimation of the LS using the outer layer truncation gives astonishingly good results even for quite small d_s. It is obvious that the truncation of the outer layer of the Jacobian has to coincide with the range of the coupling: the larger the coupling range the more outer rows and columns must be truncated. This is considered further in section VIII.

VI. LOCAL VERSUS GLOBAL FITTING: A MATTER OF DIMENSIONALITY

The technique of truncating the outer layer of the Jacobian gives outstanding results for the estimation of the LS, it does not, however, explain how such good approximations are attained. It is striking that the reconstructed LS in figure 5 are on perfect agreement with the original LS even though the embedding dimensions are a) too small to disentangle the phase space and b) too large to avoid the "curse of dimensionality". The explanation for this apparent contradiction is easy to understand since the measurement functions are the actual variables of the system, as mentioned earlier, and the form of the dynamical equations is actually contained in our basis function for the fitting. In our case, the dynamics of the CML is quadratic in nature (cf. equation (2)) and we are using a quadratic fit. Thus, the intended local fit works perfectly as a global one and therefore the problem of not finding neighbours in high-dimensions is avoided.

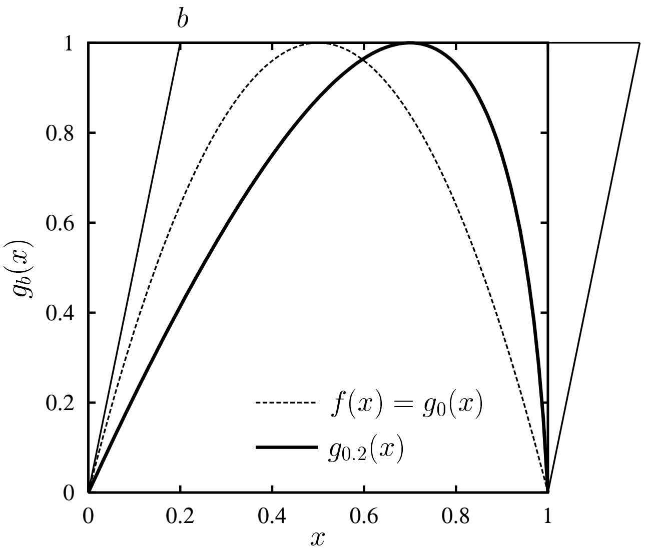

FIG. 6. Skewed logistic map (thick line) obtained by applying the skew transformation (11) to the fully chaotic logistic map (dashed line).

In a realistic situation the actual dynamics to be approximated is unlikely to be contained in the fitting basis functions. Thus, from now on, we restrict our attention to a skewed logistic local map corresponding to a CML dynamics not contained in the quadratic polynomial basis function that we use for fitting. The skewed logistic map is constructed by simply applying the following skew transformation of the unit square

$$K(x,y) = (x + by, y), \tag{11}$$

where b is the skew parameter. Applying the skew transformation (11) to the logistic map $f(x) = ax(1 - x)$ we obtain the skewed logistic map

$$g_b(x) = \frac{-1 + ab(2x-1) + \sqrt{(1+ab)^2 - 4abx}}{2ab^2}, \quad (12)$$

where the skew parameter b must satisfy $-1/a < b < 1/a$ so that the derivatives of g_b at 0 and 1 remain bounded. In figure 6 we depict the skewed logistic map for $b = 0.2$ alongside the original (non-skewed) fully chaotic logistic map.

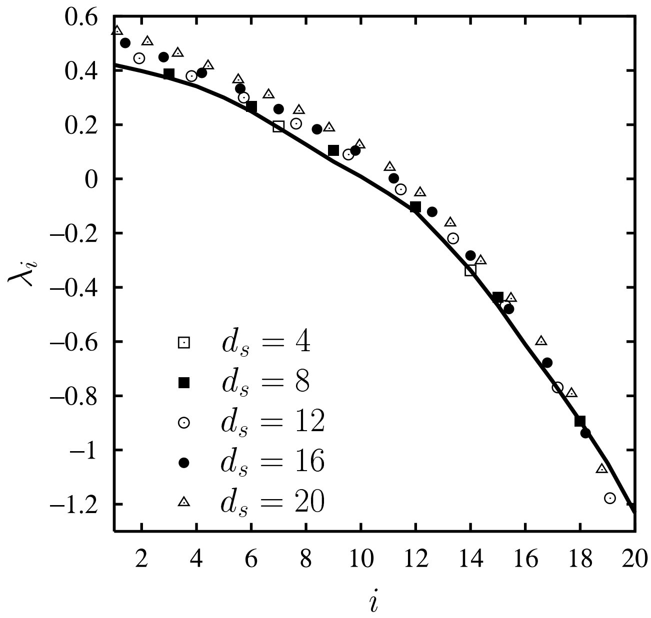

FIG. 7. Estimation of the LS for a coupled map lattice of skewed logistic maps. The size of the lattice is $N = 20$, the coupling parameter $\varepsilon = 0.4$ and the skew parameter $b = 0.2$ (*i.e.* large skew). The original LS is depicted by the line and the estimates using several spatial embedding dimensions d_s are depicted by the points. For large d_s the estimates deteriorate because of the "curse of dimensionality". All the fitting parameters are the same as in figure 2 (second order fitting, 10^4 points).

We now repeat the LS estimation depicted in figure 5 for a CML of *skewed* logistic maps. In figure 7 we show the effects of increasing the spatial embedding d_s for a large skew ($b = 0.2$) of the local map. It is interesting to notice from the figure that for small d_s (≤ 6) the approximation to the LS is quite good. However, for large d_s the approximation shifts away from the desired LS. This reflects the fact that as d_s gets larger the fitting algorithm is unable to find close neighbours for the local fit. Since now the skewed logistic map cannot be well approximated globally by a quadratic function the LS estimation deteriorates. It is worth mentioning that, even though the exact estimation of the LS is not possible in this case, the estimated LS has the right trend. This is due to the fact that the skewed logistic map still resembles a quadratic function to some extent and thus a global fitting is still reasonable. Trying a local map whose graph is not closely approximated by a quadratic leads to even greater discrepancies [4]. Note from figure 7 that the number of Lyapunov exponents for a given d_s is $d_s - 2$ due to the improved method of truncating the Jacobians outer layer. Therefore reasonable approximations achieved with $d_s \leq 6$ correspond to less than 4 points in order to approximate the whole LS. This is an obvious drawback since it is not reasonable to expect that, in general, it possible to extrapolate the whole LS by just using 4 points —this is particularly true when trying to estimate Lyapunov dimensions and entropies from LS [4]. We are therefore cursed again by the high-dimensional nature of the dynamics.

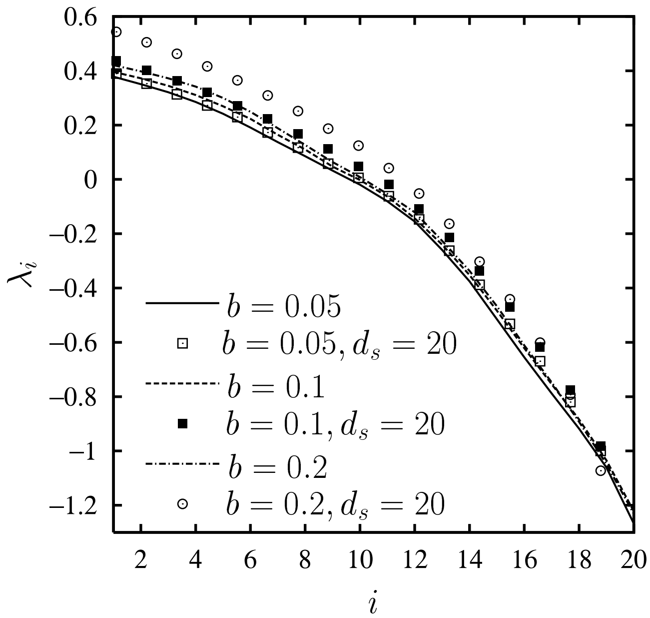

FIG. 8. Effect of the skew of the local map when estimating the LS. Lines correspond to the LS computed with the known dynamics and the points to their respective reconstruction using pure spatial delay embeddings. All the fitting parameters are the same as in figure 2 (second order fitting, 10^4 points).

Let us now compare the effects of the skew on the reconstruction of the LS. In figure 8 we plot the actual LS calculated from the known dynamics (lines) and their respective approximation using pure spatial delay embeddings with $d_s = 20$ (points) for three values of the skew parameter. For small skew ($b = 0.05$) the estimation of the LS is quite good, however, as the skew is increased, the error between the actual LS and the estimated one gets larger.

The results presented in this section would tend to suggest that as soon as the dynamics cannot be globally approximated by our basis function, and as soon as more than a handful of Lyapunov exponents is desired, it is impossible to rely on standard spatio-temporal embedding techniques to estimated the whole LS. Next section is devoted to overcome this difficulty by focusing on the reconstructing of the nontrivial entries of the Jacobian. As an alternative procedure, it is possible to use global fitting techniques by choosing a suitable basis for the fitting. By suitable basis we refer to a basis that contains the local dynamics of the extended dynamical system. This could be achieved by first extracting the local dynamics from the time series and then using this approximative local map as our fitting basis function. It is possible to partially extract the local dynamics by time-delay plots [4]. However, a much better way to obtain the local dynamics can be achieved by considering quasi-homogeneous states in a small window and their time evolution. This approach is not consider in the presented manuscript and it will be reported elsewhere [33].

VII. QUASI-DIAGONAL RECONSTRUCTION OF THE JACOBIAN

In this section we present a novel technique for estimating the Lyapunov spectrum from time series for extended dynamical systems. The method basically consists on only reconstructing the *non-zero* entries of the Jacobian. This is achieved by a row by row reconstruction of the Jacobian entries around the diagonal —here referred as quasi-diagonal reconstruction— as explained below. By doing so one avoids the problem of high-dimensionality and a large set of Lyapunov exponents can be reconstructed from a multivariate time series.

The idea behind this quasi-diagonal reconstruction of the Jacobian is quite simple. Consider the actual definition of the Jacobian matrix $J(n)$ at time n through its entries

$$J_{kl}(n) = \frac{\partial x_k^{n+1}}{\partial x_l^n}. \tag{13}$$

Due to the coupling interaction dynamics being localised, for the extended dynamical systems we consider here, many of the Jacobian entries in (13) are exactly, or at least very close to, zero. In fact, only some elements near the diagonal are different from zero, *i.e.* the Jacobian corresponds to a *banded-diagonal* matrix. In the particular case of a diffusive CML (2), there are only three diagonals of non-zero elements in the Jacobian:

$$J(n) = \begin{pmatrix} \partial_1^1 & \partial_2^1 & 0 & & & 0 \\ \partial_1^2 & \partial_2^2 & \partial_3^2 & 0 & & \\ 0 & \ddots & \ddots & \ddots & 0 & \\ & 0 & \ddots & \ddots & \ddots & 0 \\ & & 0 & \ddots & \ddots & \partial_{N_s}^{N_s-1} \\ 0 & & & 0 & \partial_{N_s-1}^{N_s} & \partial_{N_s}^{N_s} \end{pmatrix}, \tag{14}$$

where, for simplicity, $\partial_v^u = \frac{\partial x_{i_0+u-1}^{n+1}}{\partial x_{i_0+v-1}^n}$. Note that the Jacobian (14) is extracted from the sites i_0 to $i_0 + N_s - 1$ and so it is of size $N_s \times N_s$. The anchor index i_0 is not relevant because we are considering spatial homogeneity.

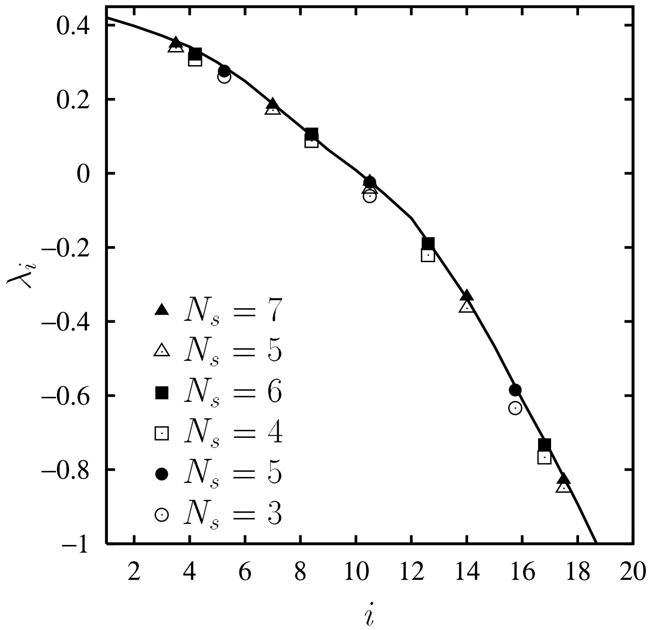

FIG. 9. Effect of truncating the outer row of the Jacobian when using the tri-diagonal reconstruction of the LS for a lattice of coupled skewed logistic maps as in figures 7 and 8. The skew is $b = 0.2$ and the width of the window where we extracted the multivariate time series is N_s sites. The open symbols correspond to using the whole fitted Jacobian while the filled symbols correspond to truncating the outer layer of the Jacobian. All the fitting parameters are the same as in figure 2 (second order fitting, 10^4 points).

Since the r-th row of the Jacobian has at most three elements different from zero around the diagonal, we can denote these elements by $J_r'(n)$ where

$$\begin{cases} J_1'(n) &= \left(\frac{\partial x_1^{n+1}}{\partial x_1^n}, \frac{\partial x_1^{n+1}}{\partial x_2^n}\right) \\ J_r'(n) &= \left(\frac{\partial x_r^{n+1}}{\partial x_{r-1}^n}, \frac{\partial x_r^{n+1}}{\partial x_r^n}, \frac{\partial x_r^{n+1}}{\partial x_{r+1}^n}\right) \\ J_{N_s}'(n) &= \left(\frac{\partial x_{N_s}^{n+1}}{\partial x_{N_s-1}^n}, \frac{\partial x_{N_s}^{n+1}}{\partial x_{N_s}^n}\right) \end{cases} \tag{15}$$

Note that for $r = 1$ and $r = N_s$ there are only two entries different from zero in the Jacobian $J(n)$ since we lack the information from outside our observed region. We can now proceed to reconstruct the whole Jacobian row by row by reconstructing each $J_r'(n)$ for increasing row index r. The number of rows in $J(n)$ is given by the size of the window (*i.e.* how many lattice nodes) where we are performing the observation of the multivariate time series *minus two*. The fact that we obtain less Lyapunov exponents than the width of our multivariate time series is analogous to the truncation of the outer layer of the Jacobian, due to boundary effects, explained in the previous section. Thus, for example, for a multivariate time series of width $N_s = 20$ sites we extract 18 Lyapunov exponents. In figure 9 we show the effects of including the truncation of the outer layer of the Jacobian. From the figure it is clear that the reconstruction using the truncation of the outer layer (filled symbols) gives consistently better results than by using the full Jacobian (open symbols). Thus, in the following, we will continue to apply the truncation of the outer layer of the Jacobian. In the next section we generalised the outer layer truncation to account for more extended couplings where the boundary effects have a larger range of interaction. It is worth mentioning that the discrepancy between these two methods used in figure 9 is less apparent as the width of our multivariate window (N_s) increases. This is consistent with the fact that the nature of the boundary effects play a lesser important role as the subsystem under consideration get larger in size [2].

Since we are only reconstructing the Jacobian around the diagonal, hence the name *quasi-diagonal reconstruction*, we can approximate the Jacobian row by row by a low dimensional map. For the r-th row ($1 < r < N_s$), at time n, the map to be approximated is

$$F_r(x_{r-1}^n, x_r^n, x_{r+1}^n) = x_r^{n+1}. \tag{16}$$

For $r = 1$ ($r = N_s$) we have the same form without the leftmost (rightmost) argument. We will, however, drop these outer-edge expressions since we will truncate the outer layer of the Jacobian anyway. So, for the inner part of the Jacobian, the map F_r depends on three variables corresponding to a diffusive coupling with nearest neighbours interaction, for other coupling interaction schemes the map F_r may depend on more variables. In order to approximate the map F_r given in (16) we have to browse our multivariate data series for close occurrences of the triplet $(x_{r-1}^n, x_r^n, x_{r+1}^n)$. An immediate advantage to this task is that, supposing spatial homogeneity, one may use *all* possible triplets in the multivariate time series provided that their spatial indexes are consecutive. Furthermore, if one assumes isotropy as well, it is possible to also use all the triplets in reverse order $(x_{r+1}^n, x_r^n, x_{r-1}^n)$. By doing so, it is possible to dramatically increase the sample set where we look for neighbours and thus increasing the chances of performing a good local approximation. However, most importantly, the quasi-diagonal reconstruction of the Jacobian relies on approximating the map F_r that only depends on *three* variables and thus the problem with high-dimensionality is avoided. Perhaps the only drawback of the quasi-diagonal method resides on the fact that it takes longer to execute. In fact, for every estimation of the Jacobian one has to perform the neighbour searching and the fitting algorithms as many times as they are rows in the Jacobian. Nevertheless, these algorithms are to be applied to triplets —not to high-dimensional vectors as before— and thus fast and effective routines may be used. For example on may use a fast neighbour searching technique described in Ref. [34].

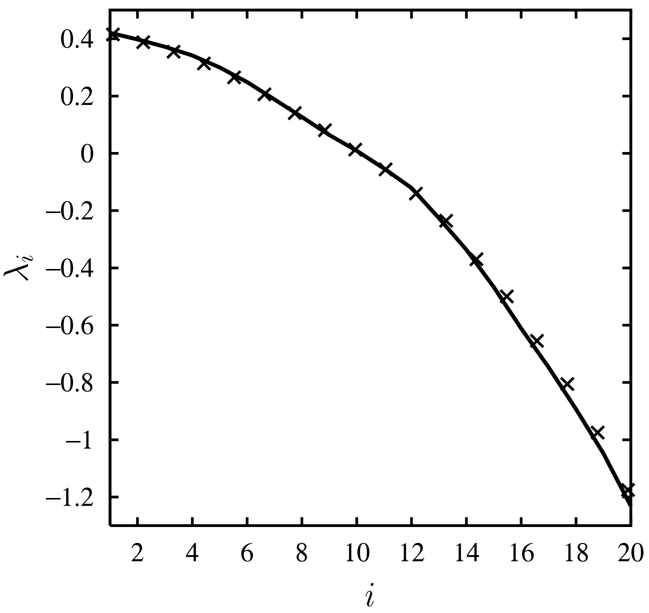

FIG. 10. Tri-diagonal reconstruction of the LS for a lattice of coupled skewed logistic maps as in figures 7 and 8. The skew is $b = 0.2$ and the width of the window where we extracted the multivariate time series is 20 sites. All the fitting parameters are the same as in figure 2 (second order fitting, 10^4 points).

In figure 10 we show an example of a LS reconstruction using the quasi-diagonal reconstruction. Compare this estimation to the ones in figures 7 and 8 where standard spatio-temporal embedding techniques previously failed. The LS is well estimated from the multivariate time series even though the local map cannot be well approximated by a quadratic fit (skewed logistic map with $b = 0.2$). Similar results where obtained for different maps and coupling strengths.

VIII. LS RECONSTRUCTION FOR DECAYING COUPLING INTERACTIONS

In the previous section we described a method to estimate the Jacobian of an spatially extended system through a tri-diagonal reconstruction. In this section we apply the quasi-diagonal method to a system where the neighbouring interaction is no longer dependent on the nearest neighbours only. In general, spatio-temporal systems, or rather the multivariate time series extracted from them, display neighbouring interactions over some finite range. These interactions are typically localised and decrease in strength for further away neighbours. For these systems, the Jacobian is no longer tri-diagonal and thus we have to modify the tri-diagonal reconstruction to allow for a wider band of non-zero elements around the diagonal. In fact, if we suppose decaying coupling interactions, the Jacobian will consist of a non-zero diagonal with sub-diagonals whose entries decay as we move away from the diagonal.

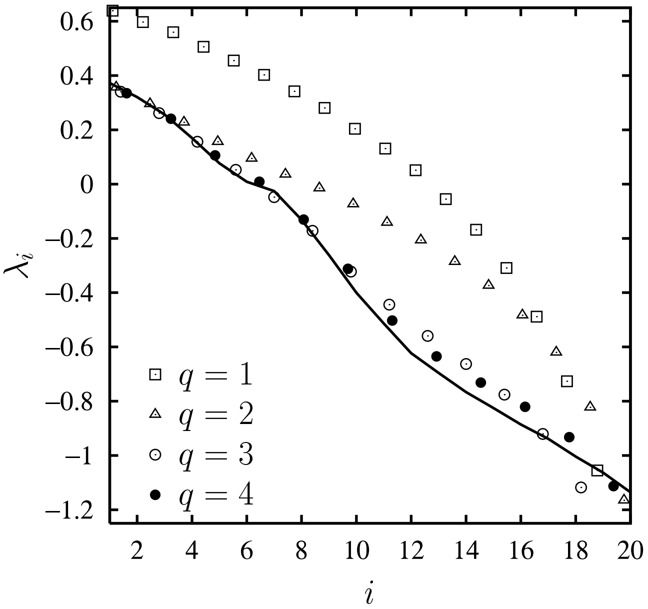

FIG. 11. Estimation of the LS using a $(2q+1)$-diagonal reconstruction of the Jacobian for a lattice of coupled skewed logistic maps with exponential decaying coupling interaction (17). The skew is $b = 0.2$ and the exponential decay rate of the interaction is $\beta = 0.35$. The coupling parameters for $\beta = 0.35$ correspond to $\varepsilon_0 \simeq 0.481$, $\varepsilon_{\pm1} \simeq 0.168$, $\varepsilon_{\pm2} \simeq 0.059$, $\varepsilon_{\pm3} \simeq 0.021$, $\varepsilon_{\pm4} \simeq 0.007$, ..., in the general CML formulation (1). All the fitting parameters are the same as in figure 2 (second order fitting, 10^4 points).

In order to model such a system let us introduce a CML where the coupling range is infinite but whose coefficients decay exponentially fast for further away neighbours. That is

$$x_i^{n+1} = \frac{e^\alpha - 1}{e^\alpha + 1} \sum_{k=-\infty}^{\infty} e^{-\alpha|i-k|} f(x_{i-k}^n),$$

where $\alpha \in (0,\infty]$ is the exponential decay and the summation coefficients were chosen in order to satisfy the conservation law $(e^\alpha - 1/e^\alpha + 1)\sum_{k=-\infty}^{\infty} e^{-\alpha|i-k|} = 1$. By defining $\beta = e^{-\alpha}$ we obtain the simpler form

$$x_i^{n+1} = \frac{1-\beta}{1+\beta} \sum_{k=-\infty}^{\infty} \beta^{|i-k|} f(x_{i-k}^n), \tag{17}$$

where now the parameter $\beta \in (0,1)$. The limit $\beta \to 0$ corresponds to the uncoupled case, *i.e.* x_i^{n+1} depends only on x_{i-k}^n. The limit $\beta \to 1$ corresponds to globally coupling all the sites with the same coefficient. Thus increasing β results on a Jacobian with more significant sub-diagonal elements further away from the main diagonal. It is obvious that for large enough β a tri-diagonal reconstruction of the Jacobian will no longer be valid and thus more sub-diagonals have to be taken into account.

Let us now, instead of using just a tri-diagonal reconstruction, try a higher-diagonal reconstruction. Thus instead of supposing that a given site only depends on the past of its nearest neighbours as in (16), let us allow this dependence to depend on further away interactions:

$$F_r^{(q)}(x_{r-q}^n \ldots, x_{r-1}^n, x_r^n, x_{r+1}^n, \ldots, x_{r+q}^n) = x_r^{n+1}, \tag{18}$$

where q fixes the size of the admissible interaction range. In fact, using $F_r^{(q)}$ allows a $(2q+1)$-diagonal reconstruction of the Jacobian. As for the tri-diagonal reconstruction, the number of Lyapunov exponents that can be extracted from the multivariate time series is less than the size of the measurement window. This is because in order to avoid boundary effects one has to truncate the borders. In the general case (18), for a multivariate time series window of width N_s sites, it is only possible to extract $N_s - 2q$ Lyapunov exponents. The results for the estimation of the LS for the new coupling scheme (17) are presented in figure 11 for different values of q. The tri-diagonal ($q = 1$) reconstruction (squares) completely fails to approximate the LS since it fails to capture the relevant sub-diagonal elements of the Jacobian. As q is increased the estimate of the LS converges towards the desired curve since the $2q+1$-quasi reconstruction of the Jacobian is able to capture more off-diagonal elements. For $q = 2$ (triangles) the largest Lyapunov exponents are well reproduced but the remaining spectrum diverges dramatically for the negative exponents. For $q = 3$ (circles) and $q = 4$ (filled circles) a quite good approximation of the LS is achieved. The positive part of the spectrum is well approximated meanwhile the negative part starts to converge to the desired value giving an excellent reconstruction of the LS. We also tried the quasi-diagonal method on other exponential decays β and local maps obtaining similar qualitative results.

IX. DISCUSSION AND GENERALISATIONS

By using a quasi-diagonal reconstruction of the Jacobian we where able to extract, with reasonable accuracy, the LS of a lattice of coupled skewed logistic maps with exponentially decaying interactions. For that example, in order to capture some of the relevant features of the Jacobians, we had to take a 9-diagonal reconstruction of the Jacobian (*i.e.* $q = 4$). It is worth mentioning that when trying higher quasi-diagonal reconstructions ($q \geq 5$) the estimation of the LS deteriorate. This is due to the recurrent problem of high-dimensionality. For $q \geq 5$ we have to find neighbours for vectors with dimension $d = 2q+1 \geq 11$ and thus the "curse of dimensionality" strikes again. We have therefore a dichotomy when trying to apply the quasi-diagonal reconstruction for systems with extended interaction: on the one hand we would like to include as many sub-diagonals as possible (*i.e.* q as large as possible), however, on the other hand, q cannot be chosen too large ($q \leq 5$) because we may have to face again the "curse of dimensionality". For an extended dynamical system whose equations of motion are unknown it is possible from the multivariate time series to give an estimation of the effects of neighbouring dynamics. This could be achieved for example through some cross correlation estimator. Once these neighbouring correlations are computed it would be possible to estimate the width of the band of the Jacobian that is most appropriate to capture the essence of these interactions.

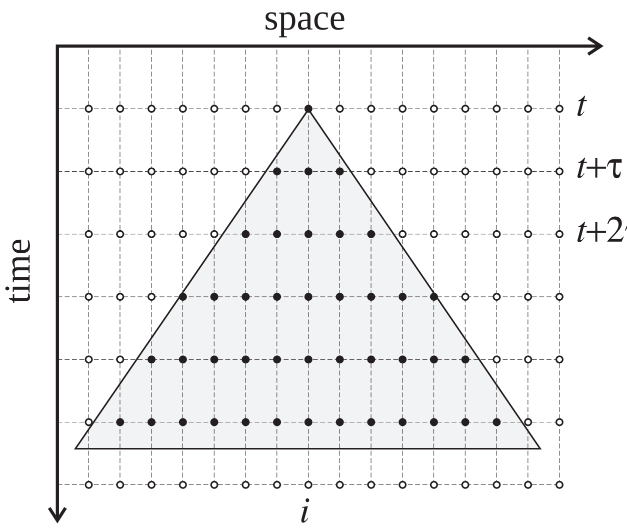

FIG. 12. Cone-horizon for a disturbance in a one-dimensional, space-time continuous, extended dynamical system. A disturbance applied at the summit of the cone may alter the downstream dynamics inside the con-horizon (shaded area). When applying a given space-time discretisation (dashed mesh) a neighbouring interaction is induced: a node at time $t+\tau$ depends on a fixed number of nodes at time t (3 in this case). The slope of the cone-horizon fixes the number of sub-diagonals to be used in the quasi-diagonal reconstruction of the Jacobians.

A related problem will arise when trying to reconstruct LS from multivariate time series produced by continuous space-time systems or when probing real life extended dynamical systems. Consider for example a one-dimensional PDE where one may choose the spatial and temporal probing lengths where the multivariate time series is to be measured. Depending on how close in space, and how often in time, we choose to probe, the Jacobian will contain a different number of significant sub-diagonals. In figure 12 we sketch the so called cone-horizon for the evolution of a perturbance in space-time. The cone-horizon corresponds to the space-time portion where a perturbance, applied at the summit of the cone, can influence downstream positions. Any point outside the cone-horizon cannot 'feel' the presence of the disturbance. These cone-horizons always exist for extended dynamical systems where the interactions have finite range, *i.e.* when information propagation in space-time has finite speed. Now suppose that we probe the system periodically in space and time. The probing corresponds to the circles placed in the intersections of the discretisation mesh (dashed lines) in the figure. Let us denote by τ the temporal sampling. We do not consider varying the spatial sampling since varying τ is enough for the illustration of our description. For the example depicted in figure 12, when the temporal sampling is equal to τ, the corresponding reconstructed Jacobian mapping from t to $t+\tau$ consists of a tri-diagonal Jacobian. This is because there are only three sites in the cone-horizon of the summit site after a time τ. Thus, for this choice of space-time discretisation it is sufficient to try a tri-diagonal reconstruction of the Jacobian ($q = 1$). However, if ones chooses 2τ as the temporal sampling (Jacobian mapping from t to $t+2\tau$), one should use a 5-diagonal reconstruction in order to include the 5 sites in the cone-horizon after a time 2τ.

At present we have not tried to apply the quasi-diagonal method to reconstruct LS from PDE. However, we are confident that our method should be able to extract some of the characteristics of the LS. This further application will be reported in a later publication.

Another important point raised by the embedding reconstruction is that in all our analysis we used the actual variables of the system as observables. Obviously, this is not commonly the case. However, we believe that a combination of the quasi-diagonal reconstruction method combined with a local spatio-temporal embedding to reconstruct the dynamics from local observables, should give reasonable results.

We would like to thank D.S. Broomhead, J. Huke and T. Schreiber for useful discussions. This work was carried out under an EPSRC grant (GR/L42513). JS would also like to thank the Leverhume Trust for financial support.

---

* E-mail: ricardo_carretero@sfu.ca
† URL: http://www.ucl.ac.uk/CNDA

[1] S. Ørstavik and J. Stark. Reconstruction and cross-prediction in coupled map lattices using spatio-temporal embedding techniques. *Phys. Lett. A*, **247** (1998) 146–160.

[2] R. Carretero-González, S. Ørstavik, J. Huke, D.S. Broomhead and J. Stark. Thermodynamic limit from small lattices of coupled maps. *Phys. Rev. Lett.*, **83** (1999) 3633–3636.

[3] M.J. Bünner and R. Hegger. Estimation of Lyapunov spectra from space-time data. *Phys. Lett. A*, **258**, 1 (1999) 25-30.

[4] S. Ørstavik, R. Carretero-González and J. Stark. Estimation of intensive measures in spatio-temporal systems

from time-series Submitted to *Physica D*, 1999.

[5] S. Lepri, A. Politi and A. Torcini. Chronotopic Lyapunov Analysis. *J. Stat. Phys.*, **82**, 5/6 (1996) 1429–1452.

[6] Y. Braiman, J.F. Lindner, W.L. Ditto. Taming spatiotemporal chaos with disorder. *Nature*, **378**, 6556 (1995) 465–467.

[7] P. Rohani and O. Miramontes. Host-parasitoid metapopulations: the consequences of parasitoid aggregation on spatial dynamics and searching efficiency. *Proc. R. Soc. Lond. B.*, **260** (1995) 335–342.

[8] Lattice Dynamics. In *Proceedings of the Workshop on Lattice Dynamics, Paris, 21–23 June 1995. Physica D*, **103**, 1997.

[9] P. Poggi and S. Ruffo. Exact solutions in the FPU oscillator chain. *Physica D*, **103** (1997) 251–272.

[10] K. Kaneko. Period-doubling of kink-antikink patterns, quasiperiodicity in anti-ferro-like structures and spatial intermittency in coupled logistic lattice. *Prog. Theor. Phys.*, **72**, 3 (1984) 480–486.

[11] I. Waller and R. Kapral. Spatial and temporal structure in systems of coupled nonlinear oscillators. *Phys. Rev. A*, **30**, 4 (1984) 2047–2055.

[12] J. Crutchfield. Space-time dynamics in video feedback. *Physica D*, **10** (1984) 229–245.

[13] D. Keeler and J.D. Farmer. Robust space-time intermittency and $1/f$ noise. *Physica D*, **23** (1986) 413–435.

[14] C. Beck. Chaotic cascade model for turbulent velocity distribution. *Phys. Rev. E*, **49**, 5 (1994) 3641–3652.

[15] K. Kaneko. Spatiotemporal chaos in one- and two-dimensional coupled map lattices. *Physica D*, **37** (1989) 60–82.

[16] K. Kaneko, editor. *Theory and applications of coupled map lattices.* John Wiley & Sons, 1993.

[17] K. Geist, U. Parlitz and W. Lauterborn. Comparison of different methods for computing Lyapunov exponents. *Prog. Theor. Phys.*, **83**, 5 (1990) 875–893.

[18] H.F. von Bremen, F.E. Udwadia and W. Proskurowski. An efficient QR based method for the computation of Lyapunov exponents. *Physica D*, **101** (1997) 1–16.

[19] J.L. Kaplan and J.A. Yorke. Chaotic behaviour of multidimensional difference equations. *Lecture Notes in Mathematics, Springer, New York*, **730** (1979) 204–227.

[20] J.-P. Eckmann and D. Ruelle. Ergodic theory of chaos and strange attractors. *Rev. Modern Phys.*, **57**, 3 (1985) 617–656.

[21] D. Ruelle. Large volume limit distribution of characteristic exponents in turbulence. *Commun. Math. Phys.*, **87** (1982) 287–302.

[22] D. Ruelle. Five turbulent problems. *Physica D*, **7** (1983) 40–44.

[23] R. Carretero-González, S. Ørstavik, J. Huke, D.S. Broomhead and J. Stark. Scaling and interleaving of subsystem Lyapunov exponents for spatio-temporal systems. *Chaos*, **9**, 2 (1999) 466–482.

[24] N. Parekh, V.R. Kumar and B.D. Kulkarni. Synchronization and control of spatiotemporal chaos using time-series data from local regions. *Chaos*, **8**, 1 (1998) 300–306.

[25] P. Collet and J.-P. Eckmann. The definition and measurement of the topological entropy per unit volume in parabolic PDE's. *Nonlinearity*, **12** (1999) 451–473.

[26] F. Takens. Detecting strange attractors in turbulence. *Lecture Notes in Mathematics*, **898** (1981) 366–381.

[27] H. Whitney. Differentiable Manifolds. *Ann. Math.*, **27** (1936) 645.

[28] T. Sauer. Private communications (1999).

[29] H. Kantz and T. Schreiber. *Nonlinear Time Series Analysis.* Cambridge Nonlinear Science series. Cambridge Univ. Press, 1998.

[30] M.R. Muldoon, D.S. Broomhead and J.P. Huke. Delay reconstruction for multiprobe signals. *IEE Digest*, **143** (1994) 3/1–3/6.

[31] L. Cao, A. Mees and K. Judd. Dynamics from multivariate time series. *Physica D*, **121** (1998) 75–88.

[32] H. Leung and T. Lo. A spatial temporal dynamical model for multipath scattering from the sea. *IEEE Transactions on Geoscience and Remote Sensing*, **33**, 2 (1995) 441–448.

[33] R. Carretero-González. Extracting local dynamics from extended dynamical systems: a times-series reconstruction perspective. In preparation, 1999.

[34] T. Schreiber. Efficient neighbor searching in nonlinear time series analysis. *Int. J. Bifurcation and Chaos*, **5**, 2 (1995) 349–358.